Jahn-Teller distortion and magnetic structure in $LaMnO_3$: A first-principles theoretical study with full structure optimizations

T. Hashimoto,[1,3] S. Ishibashi,[1,3] and K. Terakura[1,2,3]

[1]*Nanosystem Research Institute (NRI) "RICS", National Institute of Advanced Industrial Science and Technology (AIST), 1-1-1 Umezono, Tsukuba, Ibaraki 305-8568, Japan*

[2]*Research Center for Integrated Science (RCIS), Japan Advanced Institute of Science and Technology (JAIST), 1-1 Asahidai, Nomi, Ishikawa 923-1292, Japan*

[3]*JST, CREST, Kawaguchi, Saitama 332-0012, Japan*

(Received 29 December 2009; revised manuscript received 8 May 2010; published 27 July 2010; corrected 2 August 2010)

The Jahn-Teller (JT) distortion and the magnetic structure of $LaMnO_3$ were studied with first-principles theoretical calculations based on the projector augmented-wave method in generalized gradient approximation (GGA) and GGA+U. If internal coordinates and lattice constants were optimized, GGA calculations failed to predict the experimental ground state with A-type antiferromagnetic (A-AFM) ordering like in other calculations, while GGA+U calculations reproduced the experimental JT distortion and the A-AFM ground state successfully. It was also shown that a large on-site Coulomb repulsion U_{eff} on the La 4f states does not affect the results significantly.

DOI: 10.1103/PhysRevB.82.045124 PACS number(s): 75.47.Lx

I. INTRODUCTION

Manganites exhibit fascinating properties such as tunnel magnetoresistance,[1–5] colossal magnetoresistance,[6–9] etc., that can be utilized in creating new electronic devices. $LaMnO_3$ is one of the mother materials of such manganites. As a first step toward predicting device properties that include interfaces or defects, it is important to know to what extent density-functional theory (DFT) calculations can reproduce basic bulk properties of $LaMnO_3$, i.e., the Jahn-Teller (JT) distortion and the ground-state magnetic structure of the A-type antiferromagnetic (A-AFM) state. Many papers[10–14] show that if the experimental structure is used, the A-AFM state has the lowest total energy. However, if the structure is optimized for each magnetic state, predicting the ground-state magnetic structure is not a trivial task of DFT calculations.[15–20]

It was shown by Solovyev *et al.*[21] that the exchange coupling between Mn atoms is ferromagnetic (FM) in the *ab* plane irrespective of the magnitude of the JT distortion while the interlayer exchange coupling is also FM for weak JT distortion and can be AFM only with significant magnitude of the JT distortion. Note, however, that the important JT distortion in this argument is the Q_3 mode in Fig. 1(b) with the principal axis lying within the *ab* plane. Therefore, for the study of the stable magnetic ground state, the total-energy comparison is needed only between FM and A-AFM states and the key point to be addressed is whether the Q_3 JT distortion or the associated in-plane orbital ordering of alternating $(3x^2-r^2)/(3y^2-r^2)$ type can be quantitatively reproduced or not. In the study using ultrasoft pseudopotentials,[22] Sawada *et al.*[15–17] showed that the JT distortion was significantly underestimated particularly in the FM state and the A-AFM ground state was not reproduced by LDA, GGA, and LDA+U. Using the projector augmented-wave (PAW) method and GGA, and optimizing lattice constants and atomic coordinates for both A-AFM and FM states, Lorenz *et al.*[18] obtained the A-AFM ground state, although they did not show the atomic structures. On the other hand, using the same computational code and GGA of PW91,[23] Kotomin *et al.*[19] obtained FM ground state. Using the unrestricted Hartree-Fock (UHF) method and optimizing lattice constants and atomic coordinates for A-AFM state, Nicastro and Patterson[24] obtained the A-AFM ground state. However, the energy lowering of the A-AFM with respect to the FM state is relatively small, and the Mn-O-Mn angles are too large in their calculation. The underestimation of the A-AFM stability is due to the general trend that UHF method overestimates significantly the exchange splitting and reduces the strength of the superexchange. In the full-potential linearized augmented plane-wave (FLAPW) calculations, Shishidou *et al.*[20] showed that the JT distortion was reproduced semiquantitatively in LDA and GGA and even quantitatively in LDA+U if the internal coordinates were optimized with the fixed experimental lattice. However, it is rather strange that the ground-state magnetic structure was reproduced by LDA but not reproduced by GGA and LDA+U. The lattice optimization is yet to be done in their calculation.

Thus, the full structure optimization with several different approximations is worth to be done. In the present study, the full structure optimization of $LaMnO_3$ was performed in GGA and GGA+U. In the GGA calculation, if the A-AFM state was assumed, the JT distortion was qualitatively but not

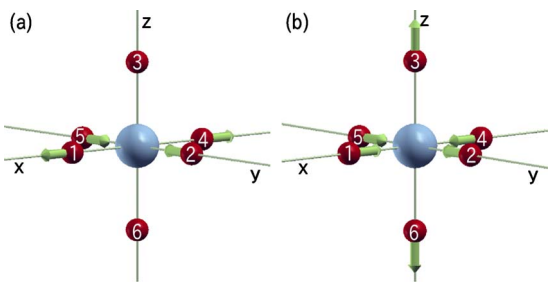

FIG. 1. (Color online) The normal mode (a) Q_2 (>0) and (b) Q_3 (>0).

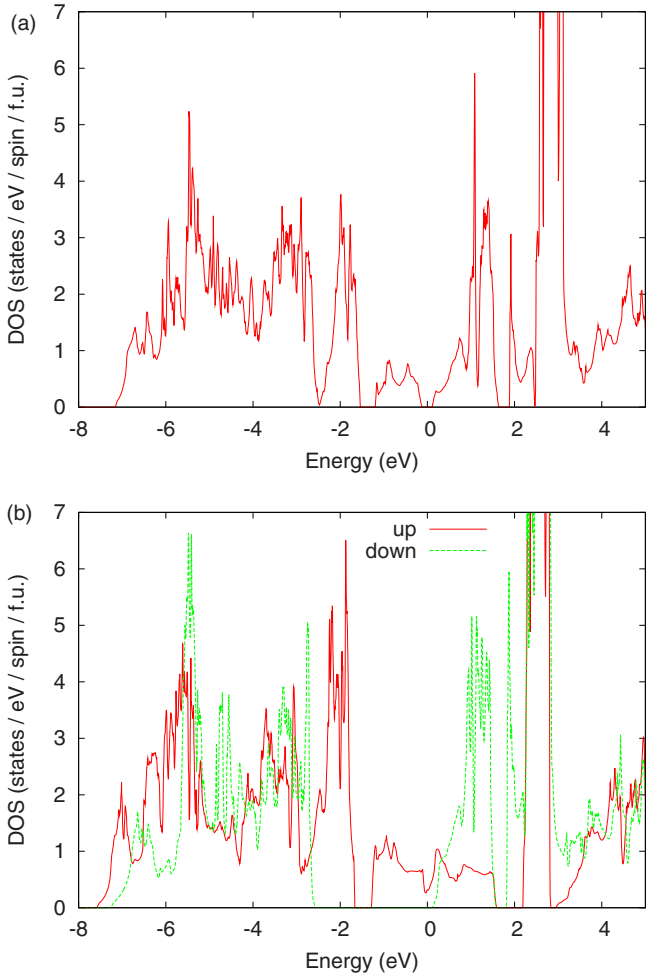

FIG. 2. (Color online) Total density of states for $LaMnO_3$ in (a) A-AFM and (b) FM states obtained in GGA for the fully optimized structure.

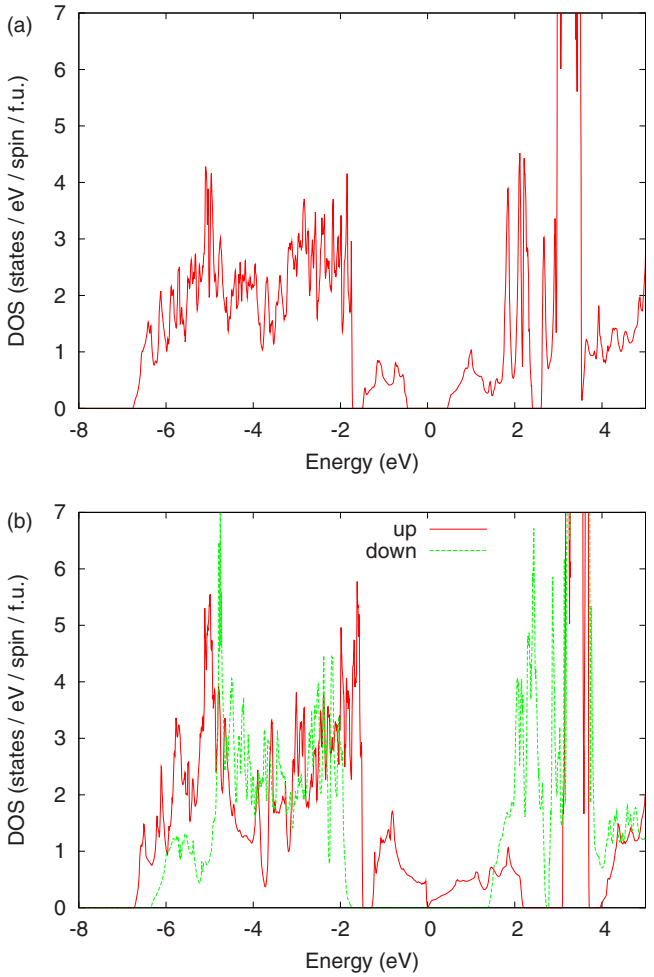

FIG. 3. (Color online) Total density of states for $LaMnO_3$ in (a) A-AFM and (b) FM states obtained in GGA+U for the fully optimized structure.

quantitatively reproduced and the ground state turned out to be FM, as in previous calculations.[15–17,19,20] In the GGA+U calculation, the JT distortion was semiquantitatively reproduced and the ground-state magnetic structure became A-AFM correctly. The failure in the GGA calculation may be attributed to serious underestimation of the alternating $(3x^2-r^2)/(3y^2-r^2)$-type in-plane orbital ordering and JT distortion in the FM state. Here we note that a similar solution for the FM state is also obtained as a metastable state in the GGA+U calculation. It was also found that applying a large on-site Coulomb repulsion U_{eff} on the La 4f states which are placed at a too low energy in DFT calculations[7,10,15,25] does not significantly change the JT distortion and the relative stability of the A-FM state. Hereafter, GGA+U(4f) means a GGA+U calculation with U_{eff} not only on Mn 3d states but also on La 4f states.

II. METHOD

The calculations are based on the PAW method.[26] The QMAS code was used in the actual calculations.[27] The GGA of the Perdew-Burke-Ernzerhof (PBE) version[28] and the GGA+U of Dudarev *et al.*[29] were used. $U_{\mathrm{eff}}=U-J$ was set to be 2 eV on Mn 3d states in GGA+U calculation. In the GGA+U(4f) calculation, U_{eff} of 14 eV was additionally introduced to La 4f states. The convergence criteria were 1×10^{-8} e/bohr^3 for the self-consistent-charge distance, 5×10^{-5} hartree/bohr for the maximum force, and 5×10^{-7} hartree/bohr^3 for the stress tensor. The plane-wave cut-off energy was set to 20 hartree. The k-space integration was performed by sampling k points with an $8\times8\times8$ uniform mesh in the Brillouin zone.[30] The Pulay stress[31–33] was included in the stress tensor to correct the effect of plane-wave cutoff on lattice constants.

III. RESULTS AND DISCUSSION

In the following, there are three levels of structural optimization: (1) no optimization and just use of experimental structure, denoted as "EXP"; (2) partial structural optimization, denoted as "P-OPT" in which only the internal coordinates are optimized with the experimental lattice constants; and (3) full structural optimization, denoted as "F-OPT." In the present GGA+U calculations, we have found some meta-

TABLE I. Calculated and experimental indirect gap, direct gap, and magnetic moment for $LaMnO_3$. Calculated results are for EXP and F-OPT structures within GGA and GGA+U.

	Experiment	Calculated			
		EXP		F-OPT	
		GGA	GGA+U	GGA	GGA+U
Indirect gap (eV)	0.24[a]	0.27	0.81	0.22	0.90
		0.278[f]		0.162[g]	
Direct gap (eV)	1.1[b]	0.70	1.18	0.61	1.20
	1.7[c]	0.677[f]			
Magnetic moment (μ_B)	3.7 ± 0.1 [d]	3.33	3.46	3.35	3.49
	3.42[e]	3.394[f]		3.46[g]	

[a]Resistivity measurements (Ref. 35).
[b]Optical measurements (Ref. 36).
[c]Photoemission measurements (Ref. 37).
[d]Neutron diffraction (Ref. 38).
[e]Neutron diffraction (Ref. 39).
[f]FLAPW method (Ref. 10).
[g]PAW method (Ref. 18).

stable solutions for the FM state. Only the lowest energy solution among them will be shown in the following two sections in order to discuss the ground-state magnetic states. The multiple solutions for the FM state will be briefly discussed in the Sec. III C.

A. Ground-state electronic structure

Before discussing the details of the crystal structures and magnetic orderings, we first show the basic electronic structures obtained by the F-OPT level calculations. The densities of states for A-AFM and FM orderings are shown in Figs. 2 and 3 calculated in GGA and GGA+U, respectively. In the calculation using ultrasoft pseudopotentials by Sawada *et al.*[15] within LDA and GGA and that by Trimarchi and Binggeli[34] within LDA, structure optimization made the ground-state A-AFM of $LaMnO_3$ metallic. In the present calculation in GGA, like in another PAW calculation,[18] this weak point is improved.

The calculated results and experimental ones for the indirect band gap, direct band gap, and magnetic moment are listed in Table I. The experimental indirect band gap was estimated by the resistivity measurement.[35] The GGA results in both EXP and F-OPT are in good agreement with the experimental one while the GGA+U results are significantly overestimated. The calculated direct band gap in GGA is less than half of the experimental data from the photoemission measurement.[37] The present GGA+U calculation with $U_{\text{eff}}=2$ eV gives still a smaller gap compared with the experimental data, but agrees well with the optical band gap.[36] However, as exciton effects were not taken into account in our calculations, this agreement is not meaningful. As for the magnetic moment, the calculated results are in reasonable agreement with the experimental values $3.7\mu_B$ (Ref. 38) and $3.42\mu_B$,[39] though the GGA results are slightly underestimated.

B. Structure and orbital ordering

In $LaMnO_3$, MnO_6 octahedra rotate and tilt due to the La-ion size that makes the tolerance factor less than one, and they distort due to the JT effect. Because of these, the b axis is elongated and the c axis is shortened with respect to the a axis.[38]

JT distortion. The local structural distortion around a Mn atom is described by normal modes Q_2 and Q_3 (Refs. 15, 40, and 41) (Fig. 1), which are represented by $Q_2=(1/\sqrt{2})(X_1-X_4-Y_2+Y_5)$ and $Q_3=(1/\sqrt{6})(2Z_3-2Z_6-X_1+X_4-Y_2+Y_5)$, where X, Y, and Z are the coordinates of the surrounding oxygen atoms with the subscript specifying the atoms. The oxygen atoms located along the principal axis are assigned to O(3) and O(6) which are lying in the ab plane in the present system.

Figures 4(a) and 5(d) show JT distortions calculated by optimizing internal coordinates with experimental lattice constants (P-OPT) and by fully optimizing both internal coordinates and lattice constants (F-OPT), respectively. Experimental results and other theoretical results are also shown. Experimentally, Q_2 and Q_3 are 0.14 a.u. and 0.78 a.u., respectively. In the level of P-OPT [Fig. 4(a)], the present GGA calculation underestimates both Q_2 and Q_3, which are 0.07 a.u. (50%) and 0.59 a.u. (75%), respectively. However, in the GGA+U calculation, they are enhanced to 0.12 a.u. (81%) and 0.68 a.u. (86%), respectively. The present PAW results for Q_2 and Q_3 are close to FLAPW results[20] for both GGA and GGA(LDA)+U calculations, and they improve the results of ultrasoft pseudopotential calculation.[15]

In the level of F-OPT [Fig. 5(d)], Q_2 and Q_3 by the GGA calculation in the A-AFM state become larger [0.09 a.u. (63%) and 0.71 a.u. (91%), respectively] and approach experimental values. Q_2 and Q_3 by the GGA+U calculation also become larger [0.12 a.u. (85%) and 0.88 a.u. (113%), respectively]. The results in GGA+$U(4f)$ are very similar to those of GGA+U: Q_2 and Q_3 are 0.13 a.u. (89%) and 0.88

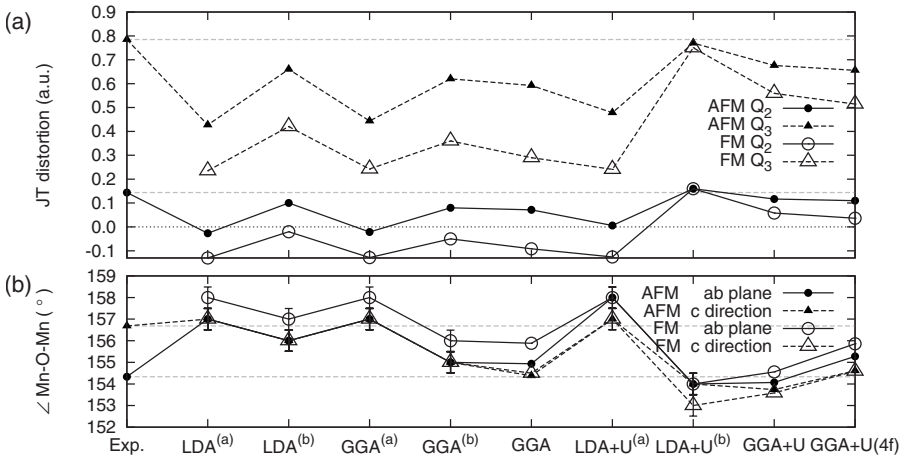

FIG. 4. (a) The JT distortion and (b) the Mn-O-Mn angles for a Mn-O-Mn pair in the *ab* plane and that along the *c* direction for the P-OPT calculations. Exp. corresponds to the experimental structure (Ref. 38). LDA[(a)], GGA[(a)], and LDA+U[(a)] correspond to the ultrasoft pseudopotential calculations (Ref. 15). LDA[(b)], GGA[(b)], and LDA+U[(b)] correspond to the FLAPW calculations (Ref. 20).

a.u. (112%), respectively. These results show that the experimental JT distortion is reproduced by GGA and GGA+U calculations semiquantitatively if the full structure optimization (F-OPT) is performed. It should be noted, however, that the volume is overestimated [Fig. 5(a)] in GGA and even more in GGA+U. As for the lattice constants, a (not shown in Fig. 5) is reproduced within about 1% in most cases while

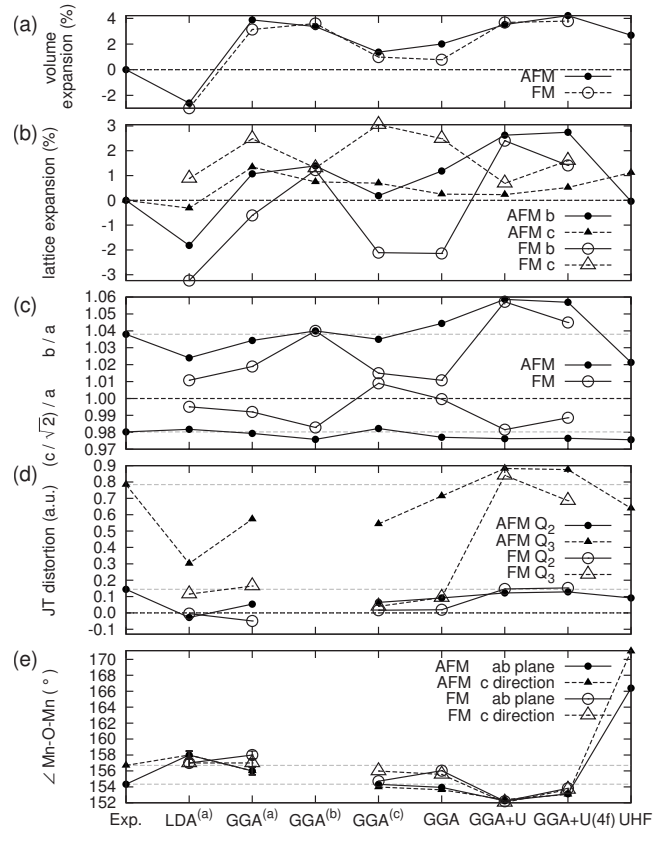

FIG. 5. (a) The volume expansion, (b) the lattice expansion, (c) the lattice constant ratios b/a and $(c/\sqrt{2})/a$, (d) the JT distortion, and (e) the Mn-O-Mn angles for a Mn-O-Mn pair in the *ab* plane and that along the *c* direction for the F-OPT calculations. Exp. corresponds to the experimental structure (Ref. 38). LDA[(a)] and GGA[(a)] correspond to the ultrasoft pseudopotential calculations (Ref. 15). GGA[(b)] and GGA[(c)] correspond to PAW calculations from Refs. 18 and 19, respectively. UHF corresponds to Ref. 24.

b may deviate from the experimental value up to about 3% as seen in Fig. 5(b). The UHF calculation[24] also semiquantitatively reproduce JT distortion [0.09 a.u. (63%) and 0.64 a.u. (82%) for Q_2 and Q_3, respectively] while the lattice constants except for b are overestimated.

Mn-O-Mn angle. The Mn-O-Mn angles for a pair of Mn-O-Mn in the *ab* plane and that along the *c* direction are shown in Figs. 4(b) and 5(e) for P-OPT and F-OPT calculations, respectively. Experimentally, the in-plane and the out-of-plane Mn-O-Mn angles are 154.3° and 156.7°, respectively. The calculated values are close to the experimental ones, except that the differences in these two angles are smaller in the present calculations as well as in the P-OPT calculation of Ref. 34. In the P-OPT calculations [Fig. 4(b)], the angles by the present calculations are very close to those by the FLAPW calculations[20] for GGA and GGA(LDA)+U. Applying $U_{\text{eff}}=14$ eV on the La $4f$ states slightly increases the Mn-O-Mn angles. In the F-OPT calculation [Fig. 5(e)], the angles become larger in the FM state for the GGA calculation, reflecting the structure with reduced JT distortions in the FM state. The UHF calculation[24] predicts very large Mn-O-Mn angles for the A-AFM ground state.

Orbital population. Figure 6 shows the orbital populations in the majority spin e_g states for $LaMnO_3$ in the EXP and F-OPT structures in GGA, GGA+U, and GGA+$U(4f)$. Here and in Fig. 6, z is taken as the local principal axis around a Mn atom. In the calculations using the experimental structure [Fig. 6(a)], the occupation number for the $3z^2-r^2$ orbital is close to one, and that for the x^2-y^2 orbital has smaller population for all the three approximations. If FM state is imposed, the occupation number for the $3z^2-r^2$ (x^2-y^2) orbital is reduced (enhanced) for all the calculations, but the system is still in the orbital ordered state.

In the fully optimized structure [Fig. 6(b)], the occupation numbers in the A-AFM state are not changed largely from those in the experimental structure. If FM state is imposed, the in-plane orbital ordering remains in GGA+U and GGA+$U(4f)$ calculations, while it almost disappears in the GGA calculation. As will be discussed in the next section, the presence of significant in-plane orbital ordering even in FM state is crucial to make A-AFM state the ground state.

La $4f$ *states.* The La $4f$ states are located by about 3 eV above the Fermi energy in the present GGA and GGA+U calculations as well as in other calculations.[7,10,15,25] Experi-

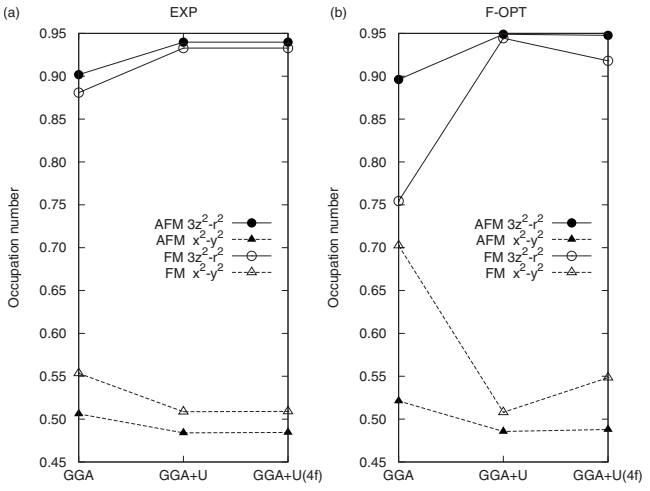

FIG. 6. The orbital population in the majority spin e_g states for $LaMnO_3$ in (a) EXP and (b) F-OPT structures within GGA, GGA $+U$, and GGA$+U(4f)$.

mentally it is located at 8.7 eV above the Fermi energy.[42] Sawada *et al.*[15] showed that if they remove the La $4f$ states artificially, the cohesion from the $2p$(O)-$4f$(La) hybridization is removed, resulting in expanded lattice constants and reduced JT distortion. Ma *et al.*[25] showed by FLAPW calculations for $La_{0.66}Sr_{0.33}MnO_3$ within LSDA$+U$ that even if a large Coulomb parameter (10 eV) is applied to the La $4f$ states, the effects on the total energy and the density of occupied states are negligible.

In the present study, $U_{\text{eff}}=14$ eV was applied to the La $4f$ orbitals so as to reproduce the experimental $4f$ level. Although the structural changes by correcting the La $4f$ levels were found to be small, there were some clear trends in the structural changes. In the level of F-OPT, the lattice constants in the A-AFM state were slightly expanded [Fig. 5(b)], and consequently, the volume expansion increased from +3.5% in GGA$+U$ to +4.2% in GGA$+U(4f)$ [Fig. 5(a)] because of the reduced $2p$(O)-$4f$(La) hybridization as discussed by Sawada *et al.*[15] If U_{eff} is applied to the La $4f$ states, the average of the eight La-O bonds was elongated by 0.02 a.u. and the average of the Mn-O-Mn angles was increased by 0.8° [Fig. 5(e)]. The bond-length elongation may correspond to the expansion of the rare-earth ion radius in ABO_3 perovskites and the present result may mimic the experimental dependence of the angle on the A-site ion radius for $AMnO_3$,[43] $ATiO_3$,[44] and $AFeO_3$,[45] which show weak B-site ion dependence.[6,46]

C. Ground-state magnetic structure

We briefly discuss the basic mechanisms of stability of the A-AFM ordering in $LaMnO_3$ following the arguments by Solovyev *et al.*[21] If there is no JT distortion and orbital ordering, the ground state is FM because the FM double exchange due to the half filling of the metallic e_g bands is stronger than the AFM superexchange due to t_{2g} orbitals. As JT distortion of Q_3 mode and $(3x^2-r^2)/(3y^2-r^2)$ type orbital ordering grow, the mechanism of the intra-ab plane Mn-Mn exchange coupling is converted from FM double exchange to FM superexchange due to the AFM-type orbital ordering. Therefore, although the basic mechanism of the magnetic coupling changes, the FM exchange coupling wins in the ab plane. On the other hand, once $(3x^2-r^2)/(3y^2-r^2)$ type orbital ordering is set in, the occupied e_g orbitals are strongly confined within the ab plane and the band gap opens. Then FM double exchange between neighboring ab planes will not operate and the AFM superexchange mediated by t_{2g} orbitals governs the inter-ab plane magnetic coupling. It is shown by Sawada *et al.*[15] that for LDA and GGA, if the hypothetical FM state is imposed, the orthorhombic lattice of $LaMnO_3$ becomes nearly cubic [Fig. 5(c)] with the JT distortions Q_2 and Q_3 approaching zero [Fig. 5(d)]. The present calculations as well as results by Kotomin *et al.*[19] within GGA also show the same trend. The strong stability of FM state in these calculations is clearly due to the weak JT distortion and the orbital ordering. However, the present GGA$+U$ calculations show a different trend. We have found some self-consistent solutions for the FM state with different degrees of JT distortion and orbital ordering. Among them, the lowest energy solution, which is lower than other metastable solutions by about 3 meV, keeps similar structure parameters (Fig. 5) to those of A-AFM with the same level of orbital ordering too (Fig. 6).[47] Other metastable solutions have more cubiclike structures with Q_3-type JT distortion reduced to about 30–40 % of the most stable FM solution. We have found at least two such metastable solutions which are nearly degenerate in energy within 0.2 meV, suggesting that the variation of total energy around the cubic FM state is very flat. This means that in the most stable FM solution, the Coulomb repulsion stabilizes the orbital ordering with a result of reducing the interplane FM exchange coupling while other metastable solutions may have stronger interplane FM exchange coupling whose energy gain is overcompensated by the reduced orbital ordering. On the other hand, between the A-AFM state and the most stable FM state, we can say that although the inclusion of local Coulomb interaction U_{eff} on Mn $3d$ orbitals may reduce the AFM superexchange[15] in a similar way to that in UHF, the destabilization of FM state due to strong orbital ordering is the main source of correct prediction of A-AFM ground state by F-OPT with GGA$+U$ and also GGA$+U(4f)$.

Figure 7 shows the total-energy difference between A-AFM and FM states $\Delta E=E_{\text{A-AFM}}-E_{\text{FM}}$ estimated by some different approximations. A negative ΔE corresponds to the experimental magnetic structure. From the ΔE, one can estimate the out-of-plane exchange integral (magnetic coupling constant) J_c using the classical spin model by $\Delta E=2J_cSS$, where $S=2$ is a spin magnetic moment of a Mn ion.

For the EXP, all the calculations predict the A-AFM ground state, although LDA$+U$ calculation by ultrasoft pseudopotentials[15,17] and by the FLAPW method[20] and the UHF calculation[24] predict very small $|\Delta E|$'s.[48] Many papers[10–14] report ΔE's obtained with experimental structures, and the estimated J_c's are summarized in Table II of Ref. 13. They are scattered because the energy difference for $LaMnO_3$ should be relatively small [Néel temperature $T_N=140$ K (Ref. 49)] and depends on computational details. The present J_c with the experimental structure in GGA$+U$ (GGA$+U(4f)$) is −1.3(−1.2) meV, and it is in good agree-

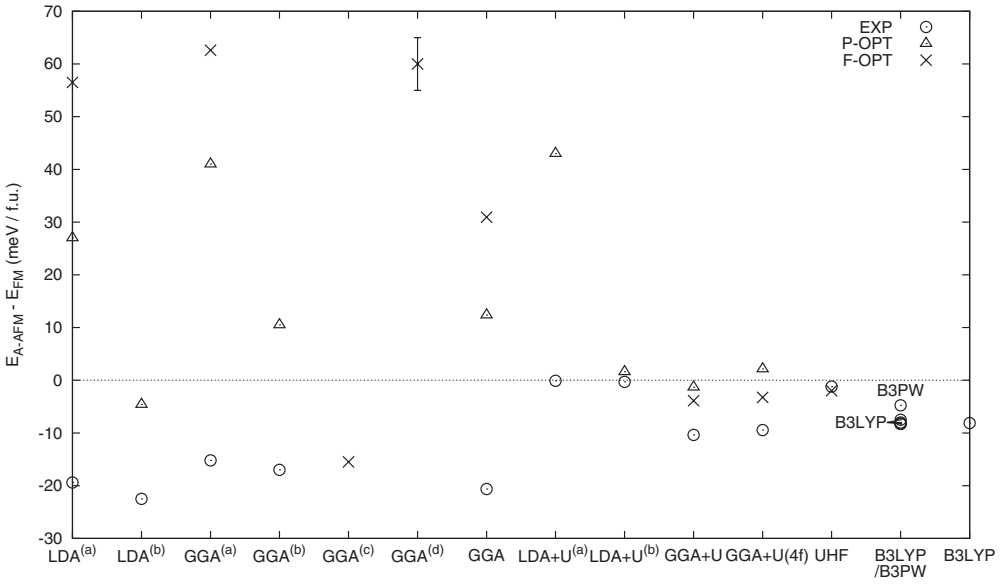

FIG. 7. The energy differences between A-AFM and FM states for $LaMnO_3$ estimated by some different approximations. $LDA^{(a)}$, $GGA^{(a)}$, and $LDA+U^{(a)}$ correspond to ultrasoft pseudopotential calculations (Refs. 15 and 17). $LDA^{(b)}$, $GGA^{(b)}$, and $LDA+U^{(b)}$ correspond to FLAPW calculations (Ref. 20). $GGA^{(c)}$ and $GGA^{(d)}$ correspond to PAW calculations from Refs. 18 and 19, respectively. UHF corresponds to Ref. 24. B3LYP/B3PW and B3LYP correspond to Refs. 13 and 14, respectively.

ment with the experimental value of −1.2 meV.[50,51]

If the internal coordinates are optimized with experimental lattice constants (P-OPT), the ΔE's become larger and in many cases become positive. The FLAPW calculations[20] and the present PAW calculations predict similar ΔE's, like in the case of the optimized structure as mentioned above.

If both the internal coordinates and the lattice constants are optimized (F-OPT), the ΔE's obtained in LDA and GGA become even more positive except for the GGA results by Lorenz *et al.*[18] On the other hand, in the present GGA+U (GGA+$U(4f)$) calculation, the A-AFM states regain their stabilities by fully optimizing the structures, resulting in $\Delta E=-3.9(-3.3)$ meV/f.u. [52] The estimated out-of-plane magnetic coupling constant is −0.5(−0.4) meV for GGA+U (GGA+$U(4f)$), which slightly underestimates the experimental value.[50,51]

IV. CONCLUSION

The full structure optimization of $LaMnO_3$ was performed by first-principles calculations using the PAW method in GGA and GGA+U. The experimental JT distortion and magnetic structure (A-AFM) were reproduced in GGA+U. In GGA calculations, the JT distortion existing in the A-AFM state was significantly reduced in the FM state, while in the GGA+U calculations, it was reproduced also in the FM state, and the A-AFM state remained to be the ground state after the full structure optimization. The present analysis suggests that the failure in the GGA calculation may be due to the strongly reduced in-plane orbital ordering in the FM state. The out-of-plane magnetic coupling constant was in agreement with experiments. Applying a large U_{eff} on the La $4f$ states does not change the JT distortion and the relative stability significantly.

ACKNOWLEDGMENTS

This work was supported by the Next Generation Supercomputer Project, Nanoscience Program, MEXT, Japan. The computations were carried out at Tsukuba Advanced Computing Center (TACC) and the facilities of the Supercomputer Center, Institute for Solid State Physics, University of Tokyo.

[1] H. Yamada, Y. Ogawa, Y. Ishii, H. Sato, M. Kawasaki, H. Akoh, and Y. Tokura, Science **305**, 646 (2004).
[2] Y. Ishii, H. Yamada, H. Sato, H. Akoh, Y. Ogawa, M. Kawasaki, and Y. Tokura, Appl. Phys. Lett. **89**, 042509 (2006).
[3] H. Zenia, G. A. Gehring, and W. M. Temmerman, New J. Phys. **9**, 105 (2007).
[4] M. Bowen, M. Bibes, A. Barthelemy, J. Contour, A. Anane, Y. Lemaitre, and A. Fert, Appl. Phys. Lett. **82**, 233 (2003).
[5] J. Z. Sun, W. J. Gallagher, P. R. Duncombe, L. Krusin-Elbaum, R. A. Altman, A. Gupta, Y. Lu, G. Q. Gong, and G. Xiao, Appl. Phys. Lett. **69**, 3266 (1996).
[6] Y. Tokura, Rep. Prog. Phys. **69**, 797 (2006).
[7] W. E. Pickett and D. J. Singh, Phys. Rev. B **53**, 1146 (1996).
[8] R. Kusters, J. Singleton, D. Keen, R. McGreevy, and W. Hayes, Physica B **155**, 362 (1989).
[9] R. von Helmolt, J. Wecker, B. Holzapfel, L. Schultz, and K. Samwer, Phys. Rev. Lett. **71**, 2331 (1993).
[10] P. Ravindran, A. Kjekshus, H. Fjellvåg, A. Delin, and O. Eriks-

son, Phys. Rev. B **65**, 064445 (2002).
[11] W. Y. Hu, M. C. Qian, Q. Q. Zheng, H. Q. Lin, and H. K. Wong, Phys. Rev. B **61**, 1223 (2000).
[12] N. Hamada, H. Sawada, I. Solovyev, and K. Terakura, Physica B **237-238**, 11 (1997).
[13] R. A. Evarestov, E. A. Kotomin, Y. A. Mastrikov, D. Gryaznov, E. Heifets, and J. Maier, Phys. Rev. B **72**, 214411 (2005).
[14] S. Piskunov, E. Spohr, T. Jacob, E. A. Kotomin, and D. E. Ellis, Phys. Rev. B **76**, 012410 (2007).
[15] H. Sawada, Y. Morikawa, K. Terakura, and N. Hamada, Phys. Rev. B **56**, 12154 (1997).
[16] H. Sawada, Y. Morikawa, N. Hamada, and K. Terakura, J. Magn. Magn. Mater. **177-181**, 879 (1998).
[17] H. Sawada and K. Terakura, Phys. Rev. B **58**, 6831 (1998).
[18] R. Lorenz, R. Hafner, D. Spišák, and J. Hafner, J. Magn. Magn. Mater. **226-230**, 889 (2001).
[19] E. A. Kotomin, R. A. Evarestov, Y. A. Mastrikov, and J. Maier, Phys. Chem. Chem. Phys. **7**, 2346 (2005).
[20] T. Shishidou, Y. Sawada, and T. Oguchi, 2006, http://ann.phys.sci.osaka-u.ac.jp/~tokutei/f_meeting/m1/jo2.pdf
[21] I. Solovyev, N. Hamada, and K. Terakura, Phys. Rev. Lett. **76**, 4825 (1996).
[22] D. Vanderbilt, Phys. Rev. B **41**, 7892 (1990).
[23] J. P. Perdew, J. A. Chevary, S. H. Vosko, K. A. Jackson, M. R. Pederson, D. J. Singh, and C. Fiolhais, Phys. Rev. B **46**, 6671 (1992).
[24] M. Nicastro and C. H. Patterson, Phys. Rev. B **65**, 205111 (2002).
[25] C. Ma, Z. Yang, and S. Picozzi, J. Phys.: Condens. Matter **18**, 7717 (2006).
[26] P. E. Blöchl, Phys. Rev. B **50**, 17953 (1994).
[27] S. Ishibashi, T. Tamura, S. Tanaka, M. Kohyama, and K. Terakura, http://qmas.jp
[28] J. P. Perdew, K. Burke, and M. Ernzerhof, Phys. Rev. Lett. **77**, 3865 (1996).
[29] S. L. Dudarev, G. A. Botton, S. Y. Savrasov, C. J. Humphreys, and A. P. Sutton, Phys. Rev. B **57**, 1505 (1998).
[30] H. J. Monkhorst and J. D. Pack, Phys. Rev. B **13**, 5188 (1976).
[31] G. P. Francis and M. C. Payne, J. Phys.: Condens. Matter **2**, 4395 (1990).
[32] P. G. Dacosta, O. H. Nielsen, and K. Kunc, J. Phys. C **19**, 3163 (1986).
[33] S. Froyen and M. L. Cohen, J. Phys. C **19**, 2623 (1986).
[34] G. Trimarchi and N. Binggeli, Phys. Rev. B **71**, 035101 (2005).
[35] R. Mahendiran, A. K. Raychaudhuri, A. Chainani, D. D. Sarma, and S. B. Roy, Appl. Phys. Lett. **66**, 233 (1995).
[36] T. Arima, Y. Tokura, and J. B. Torrance, Phys. Rev. B **48**, 17006 (1993).
[37] T. Saitoh, A. E. Bocquet, T. Mizokawa, H. Namatame, A. Fujimori, M. Abbate, Y. Takeda, and M. Takano, Phys. Rev. B **51**, 13942 (1995).
[38] J. B. A. A. Elemans, B. V. Laar, K. R. V. D. Veen, and B. O. Loopstra, J. Solid State Chem. **3**, 238 (1971).
[39] B. C. Hauback, H. Fjellvåg, and N. Sakai, J. Solid State Chem. **124**, 43 (1996).
[40] J. Kanamori, J. Appl. Phys. **31**, S14 (1960).
[41] J. H. Van Vleck, J. Chem. Phys. **7**, 72 (1939).
[42] A. Chainani, M. Mathew, and D. D. Sarma, Phys. Rev. B **47**, 15397 (1993).
[43] J. S. Zhou and J. B. Goodenough, Phys. Rev. Lett. **96**, 247202 (2006).
[44] D. A. MacLean, H. Ng, and J. E. Greedan, J. Solid State Chem. **30**, 35 (1979).
[45] M. Marezio, J. P. Remeika, and P. D. Dernier, Acta Crystallogr., Sect. B: Struct. Crystallogr. Cryst. Chem. **26**, 2008 (1970).
[46] M. Imada, A. Fujimori, and Y. Tokura, Rev. Mod. Phys. **70**, 1039 (1998).
[47] The GGA results by Lorenz *et al.* (Ref. 18) also show only small difference in lattice constants between FM and AFM states as in our GGA+U results. But the atomic structure is not shown in their paper.
[48] B3LYP calculations (Refs. 13 and 14) predict similar ΔE's with little dependence on the basis set choice and a B3PW calculation (Ref. 13) predicts a smaller absolute value.
[49] Y. Murakami, J. P. Hill, D. Gibbs, M. Blume, I. Koyama, M. Tanaka, H. Kawata, T. Arima, Y. Tokura, K. Hirota, and Y. Endoh, Phys. Rev. Lett. **81**, 582 (1998).
[50] K. Hirota, N. Kaneko, A. Nishizawa, and Y. Endoh, J. Phys. Soc. Jpn. **65**, 3736 (1996).
[51] F. Moussa, M. Hennion, J. Rodriguez-Carvajal, H. Moudden, L. Pinsard, and A. Revcolevschi, Phys. Rev. B **54**, 15149 (1996).
[52] The UHF calculation (Ref. 24) also predicts a negative ΔE of -2.0 meV/f.u.